

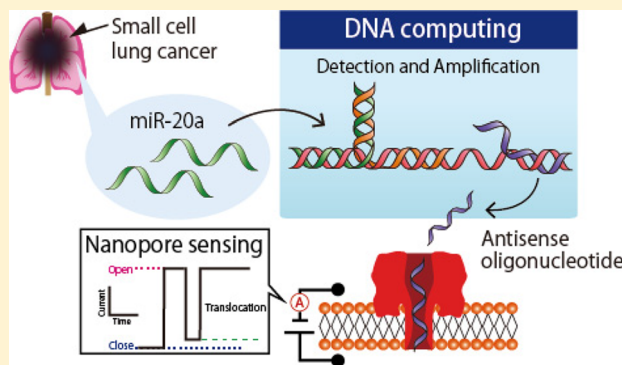
# Amplification and Quantification of an Antisense Oligonucleotide from Target microRNA Using Programmable DNA and a Biological Nanopore

Moe Hiratani, Masayuki Ohara, and Ryuji Kawano\*<sup>✉</sup>

Department of Biotechnology and Life Science, Tokyo University of Agriculture and Technology (TUAT), 2-24-16 Naka-cho Koganei-shi, Tokyo 184-8588, Japan

## Supporting Information

**ABSTRACT:** This paper describes a strategy for autonomous diagnoses of cancers using microRNA (miRNA) and therapy for tumor cells by DNA computing techniques and nanopore measurement. Theranostics, which involves the combination of diagnosis and therapy, has emerged as an approach for personalized medicine or point-of-care cancer diagnostics. DNA computing will become a potent tool for theranostics because it functions completely autonomously without the need for external regulations. However, conventional theranostics using DNA computing involves a one-to-one reaction in which a single input molecule generates a single output molecule; the concentration of the antisense drug is insufficient for the therapy in this type of reaction. Herein we developed an amplification system involving an isothermal reaction in which a large amount of the antisense DNA drug was autonomously generated after detecting miRNA from small cell lung cancer. In addition, we successfully quantified the amount of the generated drug molecule by nanopore measurement with high accuracy, which was more accurate than conventional gel electrophoresis. This autonomous amplification strategy is a potent candidate for a broad range of theranostics using DNA computing.



DNA computing is a form of molecular computing in a wet solution. Although early DNA computing studies focused on parallel and complex calculations, for example, an NP-complete problem (known as a traveling salesman problem), it has recently been demonstrated to have a broad range of applications, such as *in vivo*,<sup>1,2</sup> analytical,<sup>3</sup> and autonomous theranostic<sup>4</sup> applications. Shapiro et al. have reported<sup>4–6</sup> an autonomous diagnosis and drug release system using DNA computing as follows. “If” certain diagnostic conditions are true, such as low expression levels of certain mRNAs and high expression levels of others, “Then” the antisense drug is released. However, this type of system involves a one-to-one reaction, i.e., a single input molecule generates a single output molecule. This is incompatible with the requirement in most therapies that the concentration of the drug molecule (output) be much higher than that of the diagnostic molecule (input), so the need for amplification of the input remains a challenge.

Therapy for tumor cells is one case that matches the above scenario: first, a small amount of microRNA (miRNA) secreted from tumor cells is detected,<sup>7</sup> after which a large amount of antisense DNA to treat the tumor caused by the expression of a harmful gene is applied to the target cells. To construct a procedure to amplify an antisense drug of this kind using DNA computing, herein we focused on a DNA–enzyme isothermal reaction, in which an input molecule is obtained and used to amplify output molecules. Several isothermal amplification

methods have been proposed, among which we selected a DNA strand polymerization reaction using a nicking endonuclease and DNA polymerase.<sup>8</sup> On the basis of this amplification reaction, we constructed a theranostic system for small cell lung cancer (SCLC). In this study, we prepared a model (Figure 1): miRNA 20a (miR-20a), excreted from SCLC,<sup>9,10</sup> was detected, and then, “an oligo with the same sequence of bases as oblimersen (oblimersen)”, an antisense DNA drug,<sup>11</sup> was autonomously released with amplification. The mean concentration of exosomal miRNA from SCLC patients is 158.6 ng/mL (ca. 22.5 nM), and the dosage of oblimersen is 3 mg/kg/day (ca. 500 nmol/L/day).<sup>12</sup> Therefore, oblimersen should be amplified at an approximately 20-fold concentration from the initial miRNA concentration in this model.

To develop this autonomous system, nanopore measurement was employed to detect the output molecule in real time and without the need for labeling. The nanopore technique is a promising, recently developed method for single-molecule detection in an aqueous solution.<sup>13–18</sup> We previously demonstrated DNA logic operation in a four-droplet device including a lipid bilayer and nanopore.<sup>19</sup> The output DNA molecule was electrically detected using an  $\alpha$ -hemolysin ( $\alpha$ HL)

Received: September 29, 2016

Accepted: January 27, 2017

Published: January 27, 2017

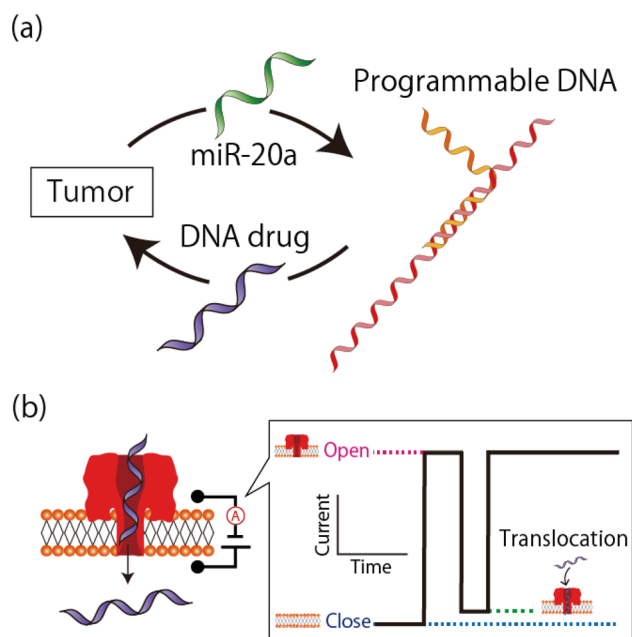


**Figure 1.** (a) Schematic illustration of the theranostic system for small cell lung cancer. (b) Schematic diagram of oblimersen translocation through the  $\alpha$ HL nanopore.

nanopore, which is utilized for the detection of single DNA/RNA molecules because the sizes of the pore and nucleotides are comparable.<sup>20–26</sup> In this droplet system, we configured outputs “1” and “0” as single-stranded DNA (ssDNA) that is or is not translocated through a nanopore, respectively; as a result, a NAND logic gate could be operated with electrical nanopore measurements. Building on this previous work, in this study, we constructed an autonomous amplification system based on DNA computing with nanopore measurements. The antisense drug oblimersen could be amplified after detecting miR-20a by isothermal amplification using a three-way junction (3WJ) structure, and then, the output molecule oblimersen was quantified by nanopore measurement, instead of by conventional gel electrophoresis.

## EXPERIMENTAL SECTION

**Reagents and chemicals.** All aqueous solutions were prepared with ultrapure water from a Milli-Q system (Millipore, Billerica, MA, USA). The reagents were as follows: 1,2-diphytanoyl-*sn*-glycero-3-phosphocholine (DPhPC; Avanti Polar Lipids, Alabaster, AL, USA), *n*-decane (Wako Pure Chemical Industries, Ltd., Osaka, Japan), and potassium chloride (KCl; Nacalai Tesque). Buffered electrolyte solutions [1.0 M KCl, 1× NE buffer 2 (New England Biolabs Japan Inc., Tokyo, Japan), pH 7.9] were prepared from ultrapure water. Wild-type alpha-hemolysin (Sigma-Aldrich, St. Louis, MO, USA, and List Biological Laboratories, Campbell, CA, USA) was obtained as the monomer polypeptide, isolated from *Staphylococcus aureus* in the form of a powder and dissolved at a concentration of 1 mg/mL in ultrapure water. For use, samples were diluted to the designated concentration using a buffered electrolyte solution and stored at 4 °C. High-performance liquid chromatography-grade DNA oligonucleotides and miRNA were synthesized by FASMAG Co., Ltd. (Kanagawa, Japan) and stored at –20 °C and –80 °C, respectively. The Klenow fragment (3′ → 5′ exo-) is an N-terminal truncation of DNA polymerase I, and it was obtained from New England

Biolabs Japan Inc. (Japan). Nt.AlwI, which is a nicking endonuclease that cleaves only one strand of DNA on a double-stranded DNA substrate, was also purchased from the same company. dNTPs were from Takara Bio Inc. (Shiga, Japan). 10× TBE buffer was obtained from Takara Bio Inc. (Japan) and was 10-fold diluted for gel electrophoresis. The power supply and an LED transilluminator were obtained from Bio Craft Co., Ltd. (Tokyo, Japan) and Optocode Corporation (Tokyo, Japan), respectively.

**DNA design and free energy calculation.** To confirm that DNA and miRNA hybridized as intended, thermodynamic analysis was performed using NUPACK (California Institute of Technology, <http://www.nupack.org/>).<sup>27</sup> Because NUPACK cannot simulate hybridization between DNA and RNA, two hybridization patterns were analyzed: between DNAs only and between RNAs only. This analysis was performed at 37 °C using a DNA or miRNA concentration of 20 nM in 1.0 M KCl-buffered electrolyte solution. The melting temperature ( $T_m$ ) was calculated with Oligo Calculator version 3.27 (Northwestern University, <http://biotools.nubic.northwestern.edu/OligoCalc.html>).<sup>28</sup>

**miRNA detection and oblimersen generation based on the three-way junction structure.** Before the enzyme reactions, the mixture of each miRNA and DNA was heated to 95 °C for 5 min and then rapidly cooled to 0 °C. miR-20a (100 nM for gel and 20 nM for nanopore experiments) was added to 10  $\mu$ L of 1× NE buffer 2 containing 20 nM primer DNA, 20 nM template DNA, 1.6 units of Klenow fragment, 4.0 units of Nt.AlwI, and 0.2 mM dNTPs. The solutions were incubated at 37 °C for 30 min for enzyme reactions. The enzyme reaction was stopped by heating at 80 °C for 20 min prior to nanopore measurements.

**Gel electrophoresis and fluorescence intensity analysis.** Products of miRNA-triggered oblimersen amplification were analyzed by 15% denaturing polyacrylamide gel electrophoresis [containing 19/1 acrylamide/bis (w/w)] in 1× TBE buffer (89 mM Tris-borate, 2 mM EDTA, pH 8.3) at a constant power of 7.5 W for 45 min at room temperature. The gel was prepared in our laboratory. After electrophoresis, the gel was stained with diluted SYBR Green II (Takara Bio Inc., Japan) solution for 30 min, imaged under blue LED irradiation, and finally imaged with a digital camera. Fluorescence intensity was analyzed by ImageJ 1.50 (National Institutes of Health, Bethesda, Maryland, USA). The fluorescence intensity of each band was calculated within square regions with the same area. The measurement of fluorescence intensity was done three times for each band.

**Bilayer lipid membrane preparation and reconstitution of  $\alpha$ -hemolysin.** Bilayer lipid membranes (BLMs) were prepared using a device produced by microfabrication. BLMs can be simultaneously formed in this device by the droplet contact method (Figure 2).<sup>29–34</sup> In this method, the two lipid monolayers contact each other and form BLMs on a parylene C film that separates two chambers. BLMs were formed as follows: the wells of the device were filled with *n*-decane (2.7  $\mu$ L) containing DPhPC (10 mg/mL). The recording solutions (4.7  $\mu$ L) on each side of the BLMs contained 1 M KCl and 1× NE buffer 2 (pH 7.9).  $\alpha$ HL was reconstituted in BLMs to form a nanopore from the ground side, and 60 nM  $\alpha$ HL was used for nanopore formation. The reaction solution was also added to the ground side. Within a few minutes of adding the solutions, BLMs were formed, and  $\alpha$ HL created nanopores within them. When the BLMs ruptured during this process, they were

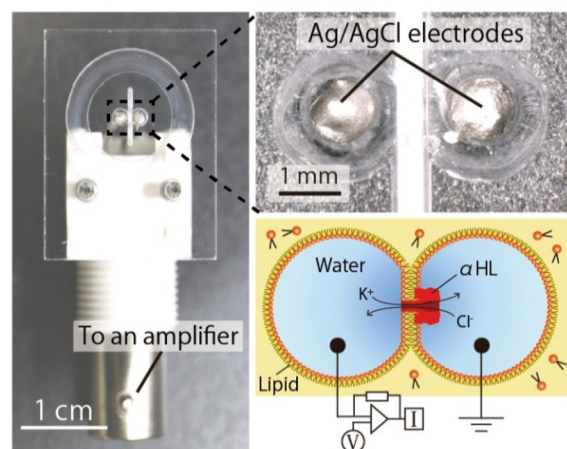


**Figure 2.** Photograph of the device for measuring channel currents. Lipid bilayers are prepared by the droplet contact method, and  $\alpha$ HL is reconstituted in the lipid bilayer.

recreated by tracing with a hydrophobic stick at the interface of the droplets.

#### Channel current measurements and data analysis.

The channel current was recorded with an Axopatch 200B amplifier (Molecular Devices, USA), filtered with a low-pass Bessel filter at 10 kHz at a sampling rate of 50 kHz, or with Pico2 (Tecella, CA, USA), filtered with a low-pass Bessel filter at 20 kHz at a sampling rate of 40 kHz. A constant voltage of +120 mV was applied from the recording side, and the ground side was grounded. The recorded data from Axopatch 200B were acquired with Clampex 9.0 software (Molecular Devices, USA) through a Digidata 1440A analog-to-digital converter (Molecular Devices, USA). The recorded data from Pico2 were monitored through TecellaLab v0.98 (Tecella, USA). Data from both amplifiers were analyzed using Clampfit 10.6 (Molecular Devices, USA), Excel (Microsoft, Washington, USA), and R software (the R Foundation). DNA or miRNA translocation and blocking were detected when >60% of open  $\alpha$ HL channel currents were inhibited. Between 200 and 500 translocating events were recorded. All data are presented as mean  $\pm$  S.E., and the differences were considered statistically significant at  $P < 0.05$  using Welch's  $t$  test. The event frequency was counted in each 10-s interval when one pore was open. Subsequently, event frequency was analyzed using the central limit theorem. Nanopore measurements were conducted at  $22 \pm 2$  °C.

## RESULTS AND DISCUSSION

**Working principle of autonomous amplification and design of DNA.** To achieve the autonomous amplification of oblimersen after discriminating miR-20a, an isothermal DNA reaction was employed using enzymes and 3WJ structure,<sup>35</sup> the structure and reaction scheme of which are shown in Figure 3. The 3WJ was formed after recognizing miR-20a and consisted of template DNA that had a sequence complementary to that of oblimersen, primer DNA, and a sequence for detecting miR-20a. Amplification was performed after the formation of the 3WJ structure as follows (see Figure 3): (i) The 3WJ structure had a site (3'-OH) for recognizing a Klenow fragment at the end of the junction, and the polymerase synthesized oblimersen along with the complementary sequence in the template DNA. (ii) Nt.AlwI that cleaves the specific site nicked the synthesized

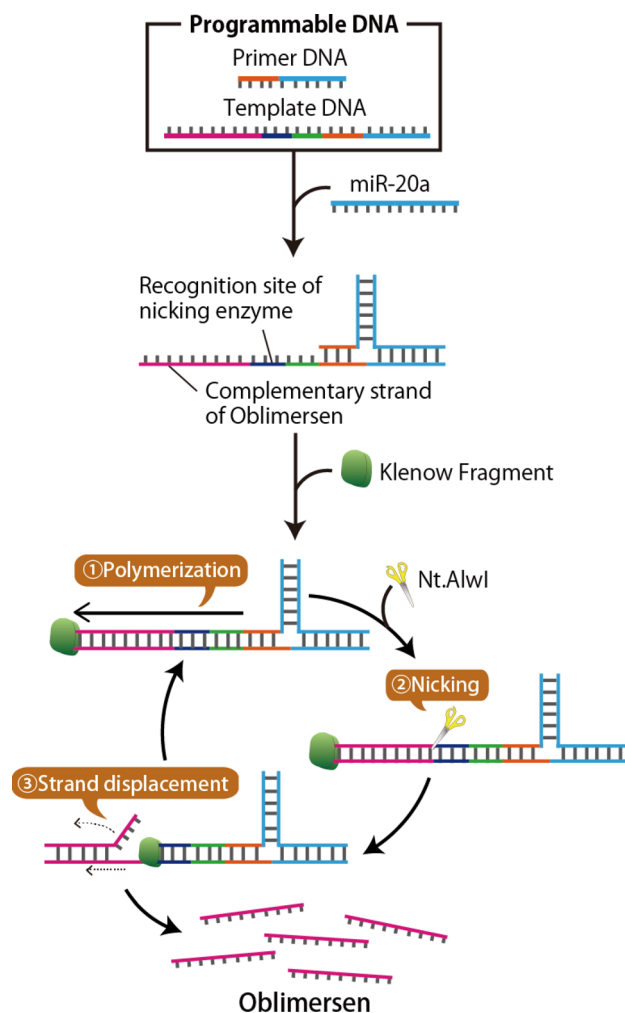


**Figure 3.** Schematic illustration of miRNA detection and oblimersen generation.

DNA to produce new 3'-OH, which induced the next polymerization by a Klenow fragment. (iii) The next polymerization started with strand displacement of oblimersen. By repeating these cycles of nicking and strand displacement, a large amount of oblimersen was autonomously generated.

Both template DNA and primer DNA contain a partial sequence complementary to miR-20a and can also join together to form double-stranded DNA. When miR-20a was not present in the solution, they did not form double-stranded structures with each other because polymerase reaction (i) undesirably occurred despite the absence of miR-20a. To design the appropriate sequence of template DNA and primer DNA, we first designed at the stem region of 3WJ because other parts were fixed as the complementary sequence of oblimersen and miR-20 (Figures 4a and 4b). Thermodynamic simulation (using NUPACK) allowed us to design a sequence associated with a  $T_m$  appropriate for the above conditions (see also the detailed protocol in the SI). The length of the stem region of the 3WJ was changed as its  $T_m$  became much lower than the reaction temperature (37 °C).<sup>35</sup> After designing the stem region, the appropriate stem sequence for the hybridization of the 3WJ structure was determined as the  $T_m$  of the stem region being 16 °C (Figure 4c). In NUPACK simulation, two different patterns needed to be stimulated, one was the 3WJ formed by DNA itself and the other was the 3WJ formed by RNA itself, because

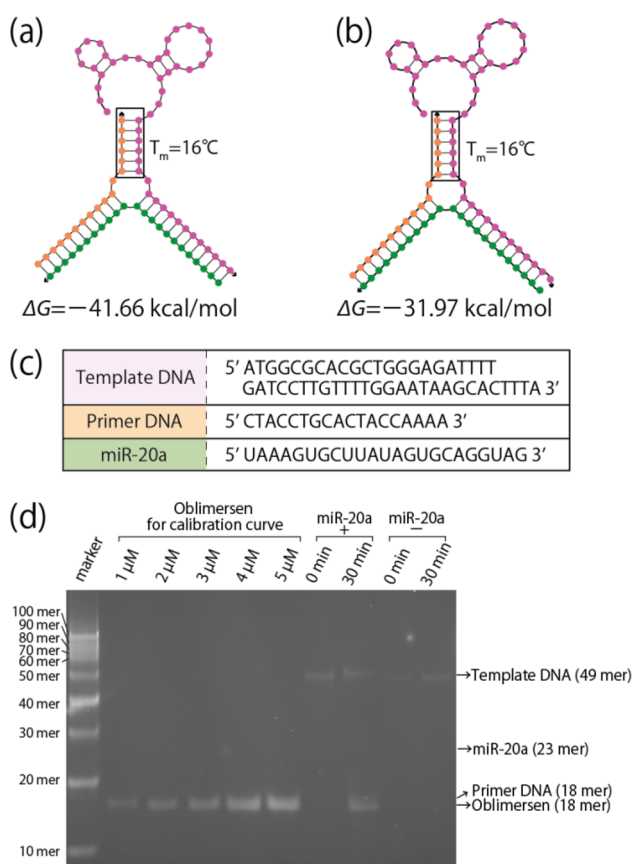


**Figure 4.** (a, b) Thermodynamic simulation of the 3-WJ predicted using NUPACK when DNA was treated as RNA (a) and when miRNA was treated as DNA (b). (c) Sequence of template DNA, primer DNA, and miR-20a. (d) PAGE image for confirmation of oblimersen generation. Products appeared in the lane of the reaction solution for 30 min in the presence of miR-20a. Lanes of oblimersen from 1  $\mu$ M to 5  $\mu$ M were used for making a calibration curve.

NUPACK cannot simulate the binding of DNA and RNA. The results of these two different simulations showed that the 3WJ structure was formed in both cases and that the  $T_m$  became the same at 16  $^{\circ}$ C. The 3WJ structure would be formed because the  $\Delta G$  of DNA–RNA hybridization becomes an intermediate value between those of DNA–DNA and RNA–RNA hybridization.<sup>36</sup> Figure 4c shows the designed 3WJ sequences, which formed a stable structure between the programmable DNA and miR-20a. The specificity of this system was verified using NUPACK simulation. The probability of 3WJ formation using the sequence similar miRNA (miR-106) was 10 times lower than that using miR-20a. Furthermore, it has been reported that hybridization cannot occur if there is a single-nucleotide difference in the miRNA structure.<sup>26</sup> The detailed procedure of the design is presented in the SI. Next, we checked the function of this design using gel electrophoresis.

#### Optimization of the isothermal reaction conditions.

Gel electrophoresis was first performed to confirm the functional capability of the primer and template DNAs. Although oblimersen was not produced when miR-20a was absent (see the lane of miR-20a “–” at 30 min in Figure 4d), a band corresponding to its molecular weight was observed in the presence of miR-20a (see the lane of miR-20a “+” at 30 min in Figure 4d), suggesting that oblimersen had been generated. In this lane, the bands for the initially added miR-20a and primer DNA were not observed because of their low concentrations

(17 nM each). Next, the reaction conditions were optimized for rapid amplification. The reaction efficiency depending on the Nt.AlwI concentration (3.0 U, 3.5 U, 4.0 U, 4.5 U, and 5.0 U) was tested because this would be the rate-limiting factor of this enzyme reaction under these conditions. The isothermal reaction showed the highest activity in the case of 4.0 U Nt.AlwI (Figure S1); similar enzyme optimization has been shown for a duplex-specific nuclease.<sup>37</sup> Finally, the quantity of oblimersen generated was examined depending on the reaction time using the fluorescence intensity of the bands. The apparent concentration of the output oblimersen was 34-fold in 30 min and 72-fold in 60 min compared with the initial concentration of miR-20a (0.1  $\mu$ M) (Figure S2). This was sufficient for the purpose of theranostics because more than 20-fold amplification from the input miRNA has been reported to be required for antisense SCLC therapy.<sup>11,12</sup> Therefore, a reaction time of 30 min was used in the nanopore experiments.

**Nanopore measurement for quantifying autonomous oblimersen generation.** An  $\alpha$ HL nanopore enables the detection of DNA or RNA electrically in real time and without the need for labeling. The nanopore was embedded in the lipid bilayer at the interface of two droplets, and it could be monitored using channel current, reflecting the translocation of the generated oblimersen from one droplet to another. Figures 5a and 5b show the typical current–time traces for the

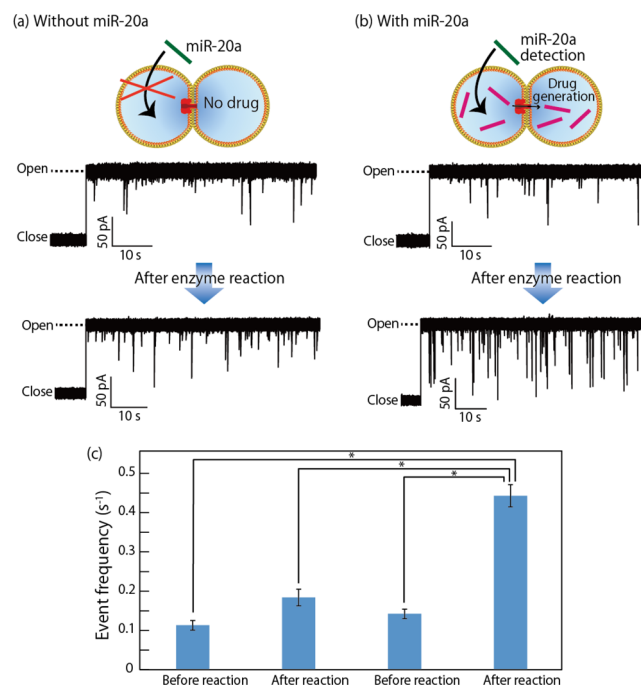


**Figure 5.** Results of nanopore measurement. (a, b) Typical current and time traces of reaction solutions before and after the enzyme reaction in the absence of miR-20a (a) and presence of miR-20a (b). (c) Event frequency for each reaction solution. Error bars indicate the standard error.

detection of output molecules before and after the enzyme reaction without and with miR-20a, respectively. In the presence of miR-20a, a number of spikelike signals were observed after the enzyme reactions, suggesting that oblimersen had been generated and passed through the nanopore. Several translocated signals were also observed in other cases because ssDNA in the initial condition, including template DNA, primer

DNA, and miR-20a, can pass through the pore. To decrease these background signals, the experimental conditions, such as the voltage applied (+120 mV) and the use of a noise filter (10 kHz), were regulated so that the translocation signal could scarcely be observed in this concentration range (approximately 20 nM). In the current recordings, the short current blockages were continually observed because of the collision (approximately 30% blockage) or the transient partial entry (approximately 60% blockage) of ssDNA into the vestibule of the  $\alpha$ HL pore.<sup>38</sup> Next, the event frequencies of each condition were compared to estimate the concentration of oblimersen generated, as shown in Figure 5c (see also the histograms in Figure S3). The translocation frequency of DNA/RNA directly reflects the concentration in the solution.<sup>23,26</sup> As shown in Figure 5c, the event frequency of oblimersen generated when miR-20a was present was clearly higher than that when miR-20a was absent. Quantification of the generated oblimersen is discussed below.

Quantitative polymerase chain reaction (qPCR) and gel electrophoresis are the conventional methods for the quantification of polynucleotides. It has been previously reported that the accuracy of qPCR for oligonucleotide quantification is lower than that of nanopore measurement.<sup>26</sup> Therefore, we examined the capability of nanopore measurement compared with that of gel electrophoresis. Although gel electrophoresis has been used as a simple quantification method in oligonucleotide quantification, its accuracy has been questioned due to the low reliability in using fluorescence intensity to determine oligonucleotide quantity. Specifically, this intensity is not consistent in each experiment, even at the same concentration; instead, it depends on factors such as the photophysical conditions. Thus, a calibration curve was created in each gel experiment by loading five different calibration samples (Figure 6a; the other calibration curves are presented in Figure S4). In the nanopore measurement, the calibration curve was established using the translocation event frequency, as mentioned above (Figure 6b). The correlation factor ( $R^2$ ) in the nanopore measurement ( $n > 3$ ) was higher than that in the gel experiment (mean  $R^2$  value of 0.82,  $n = 3$ ). In addition, the accuracy of each method was checked using a standard solution containing 3.0  $\mu$ M oblimersen. As presented in Figure 6c, the accuracy of the determined value from the nanopore measurements ( $3.0 \pm 0.26 \mu$ M,  $n = 3$ ) was higher than that from gel electrophoresis ( $2.4 \pm 2.0 \mu$ M,  $n = 3$ ). Moreover, the duration of a single experiment in the nanopore measurement was approximately 30 min, which is much shorter than that for gel electrophoresis (ca. 90 min).

Based on the results of nanopore quantification, the oblimersen concentration values before and after the enzyme reaction were determined, as depicted in Figure 6d. For the quantification of initial oligonucleotides (primer DNA, template DNA, and miR-20a) using nanopore measurement, the calibration curve from before the reaction was established (Figure S6) because the event frequency in the initial condition was varied in the case of oblimersen. After the enzyme reaction, the concentration of translocated DNA/RNA was estimated at  $550 \pm 35$  nM. The solution before the enzyme reaction contained  $86 \pm 14$  nM of the initial DNAs and miRNA. Therefore,  $460 \pm 20$  nM oblimersen was generated from 20 nM miR-20a (ca. 23-fold) in 30 min under 37 °C. The isothermal reaction with the 3WJ structure allowed us to autonomously amplify from the target miRNA to the antisense oligonucleotide.

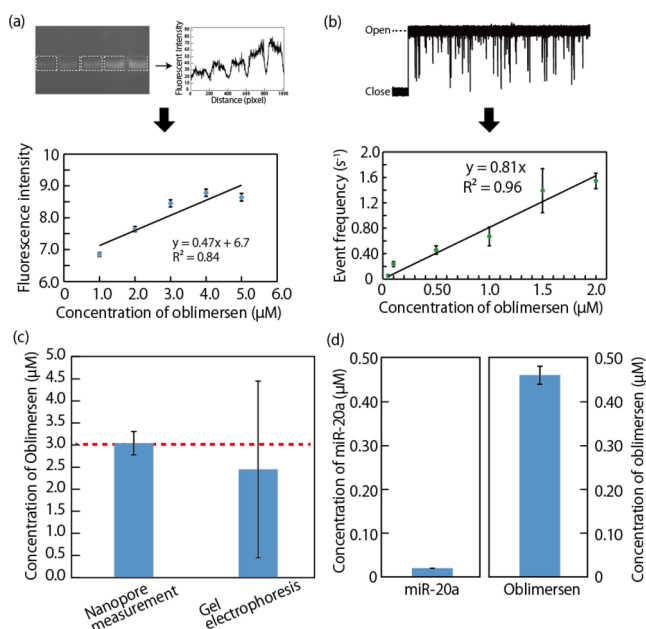


**Figure 6.** (a) Calibration curve for the estimation of oblimersen made from the fluorescence intensity in gel electrophoresis. (b) Calibration curve for the estimation of oblimersen made from the event frequency (using Axopatch 200B). (c) Estimation accuracy for 3.0  $\mu$ M oblimersen with nanopore measurement and gel electrophoresis. The calibration curve for this estimation is depicted in Figure S4 (using Pico2). Error bars indicate the standard deviation. (d) Concentrations of miR-20a and oblimersen. Error bars indicate the standard error.

## CONCLUSIONS

In summary, we developed an autonomous amplification system using DNA computing techniques. Two programmable DNA molecules, a primer and a template DNA, bound to the input miR-20a molecule and formed a 3WJ structure. After that, an isothermal reaction with enzymes was repeatedly conducted to generate a number of output oblimersen molecules. The generated oblimersen was quantified by the translocation frequency in nanopore measurement; through this experiment, we found that the quantitative capability of the nanopore measurement was greater than that using fluorescent measurement in gel electrophoresis experiments. It should thus be noted that the nanopore measurement is a more useful tool for the quantification of oligonucleotides than conventional gel electrophoresis. The results of nanopore quantification showed that oblimersen was amplified more than 20-fold from miR-20a, which meets the dosage requirement for SCLC therapy. This autonomous amplification strategy is a potent candidate for a broad range of theranostics with antisense oligonucleotides.

## ASSOCIATED CONTENT

### Supporting Information

The Supporting Information is available free of charge on the ACS Publications website at DOI: 10.1021/acs.analchem.6b03830.

Design protocol of template and primer DNA, gel electrophoresis data for the optimization of enzyme reaction, histograms of the event frequency of oblimersen in nanopore measurements, and calibration curves of the quantification of oligonucleotides (PDF)

## AUTHOR INFORMATION

## Corresponding Author

\*E-mail: rjkawano@cc.tuat.ac.jp.

## ORCID

Ryuji Kawano: 0000-0001-6523-0649

## Author Contributions

M.H. and R.K. conceived the original idea and wrote the paper. M.H. and M.O. conducted the experiments. All authors have given approval to the final version of the manuscript.

## Notes

The authors declare no competing financial interest.

## ACKNOWLEDGMENTS

We thank M. Takinoue (Tokyo Tech.) for a useful discussion on the design of the 3WJ structure. This work was partially supported by KAKENHI (Molecular Robotics: No. 15H00803 and No. 16H06043) from MEXT Japan.

## REFERENCES

- (1) Kahan-Hanum, M.; Douek, Y.; Adar, R.; Shapiro, E., A library of programmable DNazymes that operate in a cellular environment. *Sci. Rep.* **2013**, 3.10.1038/srep01535
- (2) Culler, S. J.; Hoff, K. G.; Smolke, C. D. *Science* **2010**, 330 (6008), 1251–1255.
- (3) Jung, C.; Ellington, A. D. *Acc. Chem. Res.* **2014**, 47 (6), 1825–1835.
- (4) Benenson, Y.; Gil, B.; Ben-Dor, U.; Adar, R.; Shapiro, E. *Nature* **2004**, 429 (6990), 423–429.
- (5) Shapiro, E.; Gil, B. *Science* **2008**, 322 (5900), 387–388.
- (6) Benenson, Y.; Paz-Elizur, T.; Adar, R.; Keinan, E.; Livneh, Z.; Shapiro, E. *Nature* **2001**, 414 (6862), 430–434.
- (7) Schwarzenbach, H.; Hoon, D. S. B.; Pantel, K. *Nat. Rev. Cancer* **2011**, 11 (6), 426–437.
- (8) Komiya, K.; Yamamura, M. *New Generation Computing* **2015**, 33 (3), 213.
- (9) Rabinowitz, G.; Gercel-Taylor, C.; Day, J. M.; Taylor, D. D.; Kloecker, G. H. *Clin. Lung Cancer* **2009**, 10 (1), 42–46.
- (10) Ebi, H.; Sato, T.; Sugito, N.; Hosono, Y.; Yatabe, Y.; Matsuyama, Y.; Yamaguchi, T.; Osada, H.; Suzuki, M.; Takahashi, T. *Oncogene* **2009**, 28 (38), 3371–3379.
- (11) Rudin, C. M.; Kozloff, M.; Hoffman, P. C.; Edelman, M. J.; Karnauskas, R.; Tomek, R.; Szeto, L.; Vokes, E. E. *J. Clin. Oncol.* **2004**, 22 (6), 1110–1117.
- (12) Rudin, C. M.; Otterson, G. A.; Mauer, A. M.; Villalona-Calero, M. A.; Tomek, R.; Prange, B.; George, C. M.; Szeto, L.; Vokes, E. E. *Annals of Oncology* **2002**, 13 (4), 539–545.
- (13) Bayley, H.; Cronin, B.; Heron, A.; Holden, M. A.; Hwang, W. L.; Syeda, R.; Thompson, J.; Wallace, M. *Mol. BioSyst.* **2008**, 4 (12), 1191–208.
- (14) Taniguchi, M. *Anal. Chem.* **2015**, 87 (1), 188–199.
- (15) Ying, Y.-L.; Zhang, J.; Gao, R.; Long, Y.-T. *Angew. Chem., Int. Ed.* **2013**, 52 (50), 13154–13161.
- (16) Stoloff, D. H.; Wanunu, M. *Curr. Opin. Biotechnol.* **2013**, 24 (4), 699–704.
- (17) Reiner, J. E.; Balijepalli, A.; Robertson, J. W. F.; Campbell, J.; Suehle, J.; Kasianowicz, J. J. *Chem. Rev.* **2012**, 112 (12), 6431–6451.
- (18) Deamer, D. *Annu. Rev. Biophys.* **2010**, 39, 79–90.
- (19) Yasuga, H.; Kawano, R.; Takinoue, M.; Tsuji, Y.; Osaki, T.; Kamiya, K.; Miki, N.; Takeuchi, S. *PLoS One* **2016**, 11 (2), e0149667.
- (20) Deamer, D. W.; Branton, D. *Acc. Chem. Res.* **2002**, 35 (10), 817–825.
- (21) Meller, A.; Nivon, L.; Brandin, E.; Golovchenko, J.; Branton, D. *Proc. Natl. Acad. Sci. U. S. A.* **2000**, 97 (3), 1079–1084.
- (22) Kasianowicz, J. J.; Brandin, E.; Branton, D.; Deamer, D. W. *Proc. Natl. Acad. Sci. U. S. A.* **1996**, 93 (24), 13770–13773.
- (23) Kawano, R.; Osaki, T.; Sasaki, H.; Takinoue, M.; Yoshizawa, S.; Takeuchi, S. *J. Am. Chem. Soc.* **2011**, 133 (22), 8474–8477.
- (24) Ohara, M.; Sekiya, Y.; Kawano, R. *Electrochemistry* **2016**, 84 (5), 338–341.
- (25) Zhang, X. Y.; Wang, Y.; Fricke, B. L.; Gu, L. Q. *ACS Nano* **2014**, 8 (4), 3444–3450.
- (26) Wang, Y.; Zheng, D. L.; Tan, Q. L.; Wang, M. X.; Gu, L. Q. *Nat. Nanotechnol.* **2011**, 6 (10), 668–674.
- (27) Zadeh, J. N.; Steenberg, C. D.; Bois, J. S.; Wolfe, B. R.; Pierce, M. B.; Khan, A. R.; Dirks, R. M.; Pierce, N. A. *J. Comput. Chem.* **2011**, 32 (1), 170–173.
- (28) Kibbe, W. A. *Nucleic Acids Res.* **2007**, 35, W43–W46.
- (29) Watanabe, H.; Kawano, R. *Anal. Sci.* **2016**, 32 (1), 57–60.
- (30) Kawano, R.; Tsuji, Y.; Kamiya, K.; Kodama, T.; Osaki, T.; Miki, N.; Takeuchi, S. *PLoS One* **2014**, 9 (7), e102427.
- (31) Tsuji, Y.; Kawano, R.; Osaki, T.; Kamiya, K.; Miki, N.; Takeuchi, S. *Anal. Chem.* **2013**, 85 (22), 10913–10919.
- (32) Tsuji, Y.; Kawano, R.; Osaki, T.; Kamiya, K.; Miki, N.; Takeuchi, S. *Lab Chip* **2013**, 13 (8), 1476–1481.
- (33) Kawano, R.; Tsuji, Y.; Sato, K.; Osaki, T.; Kamiya, K.; Hirano, M.; Ide, T.; Miki, N.; Takeuchi, S. *Sci. Rep.* **2013**, 3, 1995.
- (34) Kawano, R.; Osaki, T.; Sasaki, H.; Takeuchi, S.; Polymer-Based Nanopore-Integrated, A. *Small* **2010**, 6 (19), 2100–2104.
- (35) Zhang, Q.; Chen, F.; Xu, F.; Zhao, Y. X.; Fan, C. H. *Anal. Chem.* **2014**, 86 (16), 8098–8105.
- (36) Nakano, S.; Fujimoto, M.; Hara, H.; Sugimoto, N. *Nucleic Acids Res.* **1999**, 27 (14), 2957–2965.
- (37) Lv, W. F.; Zhao, J. M.; Situ, B.; Li, B.; Ma, W.; Liu, J. M.; Wu, Z. X.; Wang, W.; Yan, X. H.; Zheng, L. *Biosens. Bioelectron.* **2016**, 83, 250–255.
- (38) Akeson, M.; Branton, D.; Kasianowicz, J. J.; Brandin, E.; Deamer, D. W. *Biophys. J.* **1999**, 77 (6), 3227–3233.